International Journal of Engineering Research & Technology (IJERT)
ISSN: 2278-0181
Vol. 7 Issue 05, May-2018

Numerical Analysis of Transonic Airfoil

Dhruva Koti
M. Tech Student,
Aeronautical Engineering Department
MVJ College of Engineering
Bangalore, Karnataka, India

Ayesha Khan M.
Asst. Professor,
Aeronautical Engineering Department
MVJ College of Engineering
Bangalore, Karnataka, India

***Abstract*— The presence of shock waves over the airfoil surfaces in transonic flows leads to degraded performance. However supercritical airfoils are designed to reduce this loss of performance. RAE 2822 airfoil is a supercritical airfoil which is designed to have a roof-top type pressure distribution. Numerical simulations of transonic flow over the RAE2822 airfoil have been carried out. The objective of the paper is to study the flow over supercritical airfoil. Numerical analysis has been carried using Ansys 16.0. A grid independence study has been carried out and the results have been compared with experimental results. The Mach number contour and velocity contour show the effect of shock wave on the flow over airfoil.**

***Keywords*— Supercritical Airfoil, Transonic Flow**

I. INTRODUCTION

As the speed of aircraft increases beyond the critical Mach number, the local flow over some parts of the aircraft becomes supersonic. This type of flow is referred to as transonic flow where it behaves locally supersonic. As a result of local supersonic flow, shock waves occur on an airfoil which leads to a degradation of the performance. These shock waves get stronger with increase in freestream Mach number. The shock leads to a rapid increase in drag with increase in Mach number. To counter this problem supercritical airfoils are designed. The supercritical airfoils are characterized by large leading-edge radius, flatter upper surface instead of curvature and high camber near the aft of the airfoil. Key elements of supercritical airfoils are (1) A large radius at the leading edge that expands the flow on the upper surface leading edge. This gives a higher lift as compared to previous airfoil designs. (2) A flatter upper surface which gives almost constant pressure on the upper surface in the supersonic flow region and leads to almost constant or reduced flow speed. A relatively weak shock is formed by reducing the flow speed going into the shock. (3) Another means of obtaining lift without strong shocks at transonic speed is to use aft camber. A higher aft camber generates more lift than a low camber. The higher lift in combination with reduced shock strength lead to a better aerodynamic performance. The supercritical airfoils have a significantly higher drag divergence Mach number.

The RAE 2822 airfoil (Fig.1) is chosen for analysis as it is a supercritical airfoil. It has a sharp trailing edge in addition to the characteristics of supercritical airfoil mentioned above. The airfoil has a roof top type pressure distribution at design conditions and is designed using a second order method. The maximum thickness of the airfoil is 12.1% at 37.9% of chord length and the maximum camber is 1.3% at 75.7% of chord. The characteristics of the airfoil are mentioned in Table 1.

TABLE I. AIRFOIL CHARACTERISTICS

Property	Value
Airfoil Designation	RAE 2822
Nose Radius	0.00827c
Maximum Thickness	0.121c
Base Thickness	0
Maximum Camber	0.013c
Design Conditions	M=0.66 C_L=0.56 at α=1.06°

Fig. 1 RAE 2822 airfoil section

II. GOVERNING EQUATIONS

Computational Fluid Dynamics is governed by conservation of mass, momentum and energy equations. Conservation of mass is given by the continuity equation (1). Thus, it means that the rate at which mass enters the system is equal to the rate at which it exits the system.

$$\frac{\partial \rho}{\partial t} + \frac{\partial}{\partial x_j}(\rho U_j) = 0 \qquad (1)$$

For viscous flows the Navier Stokes equations are used and in case of turbulent flows the time-averaged Navier Stokes equations called the Reynold's Averaged Navier Stokes equations are used. The Navier Stokes equations along with the continuity equation and energy conservation equation are used for the analysis of fluid dynamics problem. The x-component of Navier Stokes equation is given by (2).

$$\frac{\partial}{\partial t}(\rho U_i) + \frac{\partial}{\partial x_j}(\rho U_i U_j) = -\frac{\partial p}{\partial x_i} + \frac{\partial \tau_{ij}}{\partial x_j} \qquad (2)$$

The energy equation given by (3) basically states that the energy of the system is conserved. In case of fluid flows, the rate of work done and rate of heat transfer into the control volume is equal to the change in energy of the system.

$$\frac{\partial}{\partial t}(\rho h) + \frac{\partial}{\partial x_j}(\rho U_j h) = \frac{\partial p}{\partial t} + U_j \frac{\partial p}{\partial x_j} + \tau_{ij} \frac{\partial U_j}{\partial x_j} - \frac{\partial q_i}{\partial x_i} \qquad (3)$$

International Journal of Engineering Research & Technology (IJERT)
ISSN: 2278-0181
Vol. 7 Issue 05, May-2018

III. METHODOLOGY

Pointwise software was used for modelling of the airfoil and grid generation. The airfoil co-ordinates were taken from [1] and imported into pointwise and a structured grid was generated. The chord length of the airfoil is taken to be 1m. The domain size for the grid is 30 times the chord length on all sides as shown in Fig 2. The grid is refined near the surface of the airfoil as shown in Fig 3. There is further refinement of grid near the leading and trailing edge of the airfoil as shown in Fig 4 and 5. The complete generated grid is shown in Fig. 6. ANSYS 16.0 was used for simulating the flow over the airfoil. The grid details are given in Table 2. The solver chosen was Fluent which is based on the finite volume method. The density-based solver was used and the turbulence model used is Realizable k-ε model with enhanced wall functions. The input boundary conditions are given in Table 3.

TABLE II. GRID DETAILS

Grid Parameter	Value
Skewness	0-0.133
Average Skewness	0.039
Orthogonal Quality	0.732-1
Average Orthogonal Quality	0.906
Y+ value	< 3

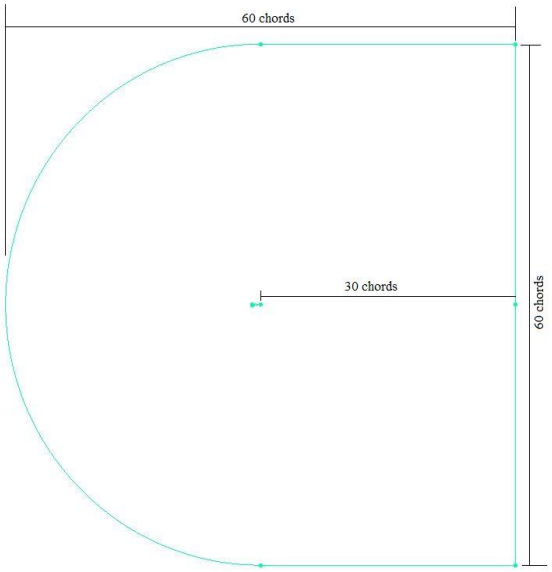

Fig. 2 Computational Domain

TABLE III. BOUNDARY CONDITIONS

Boundary Name	Boundary Type	Condition
Airfoil	Wall	V=0
Farfield	Pressure Far field	M=0.725 Re= 6.5 million α = 2.92°

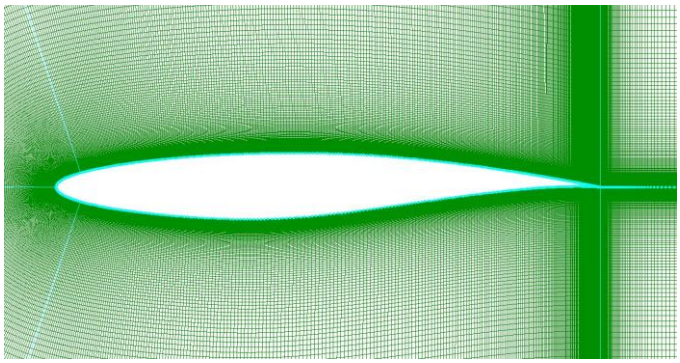

Fig. 3 Grid around the airfoil

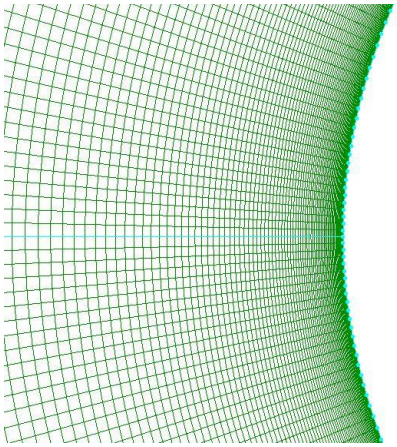

Fig. 4 Grid distribution near the leading edge

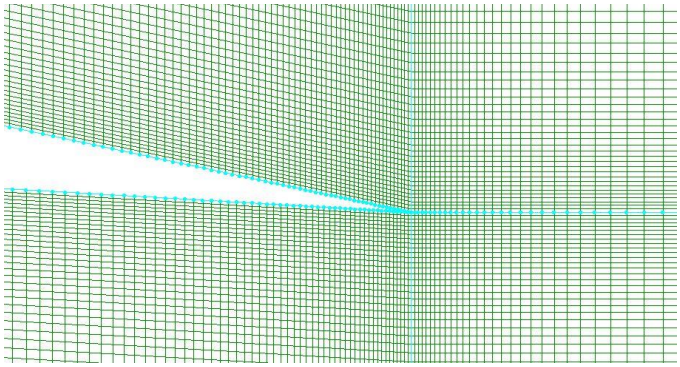

Fig. 5 Grid distribution near trailing edge

International Journal of Engineering Research & Technology (IJERT)
ISSN: 2278-0181
Vol. 7 Issue 05, May-2018

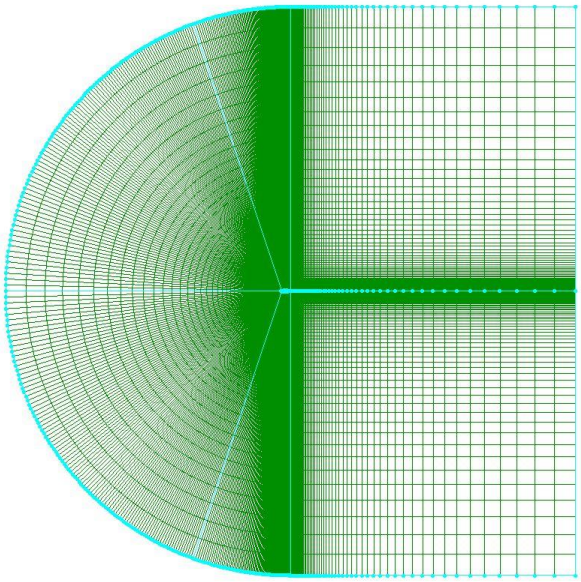

Fig. 6 Generated grid in Pointwise

IV. RESULT AND DISCUSSION

Numerical simulations for three different grid sizes (1.85 lakh, 2.97 lakh, 4.46 lakh) were carried out and their pressure coefficients were compared in order to do mesh independent study. Fig 7 shows the variation of pressure coefficient over the airfoil for the different grids. The pressure coefficient distribution Case 2(2.97 lakh) and Case 3(4.46 lakh) match well with each other. A comparison of the numerical results with the experimental results [1] was also done. Table 4 shows the comparison of lift and drag coefficients with the experimental results. The lift and drag coefficients of numerical results are very close to the experimental results and it can be noted that Case 3 grid gives the least error. The pressure coefficient plot in Fig 7 is also compared with the experimental result and the numerical results are in good agreement with the experimental result. It is observed that the numerical simulations predicted the shock location slightly upstream of the experimental location. The major reason for this is that during numerical analysis it is assumed that the flow is fully turbulent while for the experimental analysis a transition trip is used for transitioning flow from laminar to turbulent near the leading edge. Discretization errors also contribute to the slight mismatch of the plot.

TABLE IV. LIFT AND DRAG COEFFICIENT COMPARISON

Case	Grid Size	Lift Coefficient	Drag Coefficient
Experiment	-	0.743	0.0127
Case 1	1.85 lakh	0.7367	0.01294
Case 2	2.97 lakh	0.7384	0.01285
Case 3	4.46 lakh	0.7385	0.01274

The pressure contour (Fig. 8) shows the variation of pressure over the airfoil. It can be noted that there is a sudden drop of pressure just downstream of the leading edge. But further downstream, the pressure is almost constant upto 50% of chord length. This confirms with the roof-top type pressure distribution at design conditions. It can also be observed that there is an adverse pressure gradient at 50% of chord.

From the Mach number contour (Fig. 9), it can be observed that the Mach number and the velocity over the upper surface of the wing decreases as the flow progresses downstream. The Mach number contour agrees with the pressure coefficient plot. Further it can be observed that there is a sudden velocity drop at about 50% of chord length. It indicates the presence of a shock. Fig. 10 shows velocity contour which agrees with the Mach number contour which ascertains the presence of shock at about 50% of chord length.

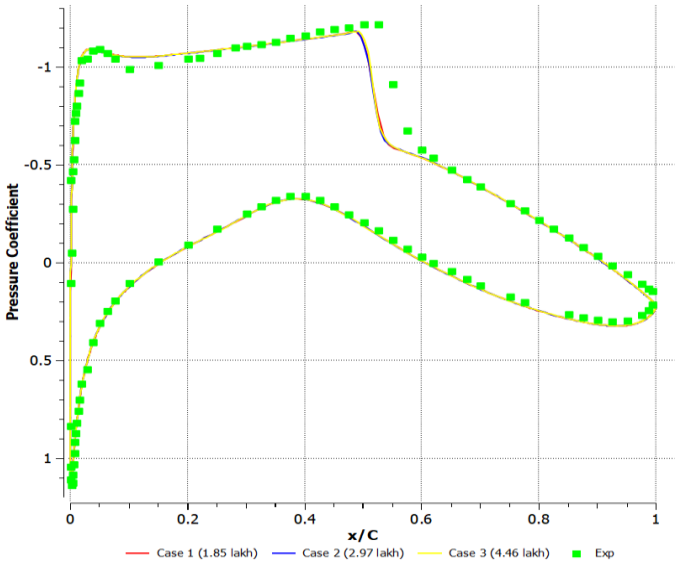

Fig. 7 Pressure Coefficient plot distribution showing the results of grid independence study

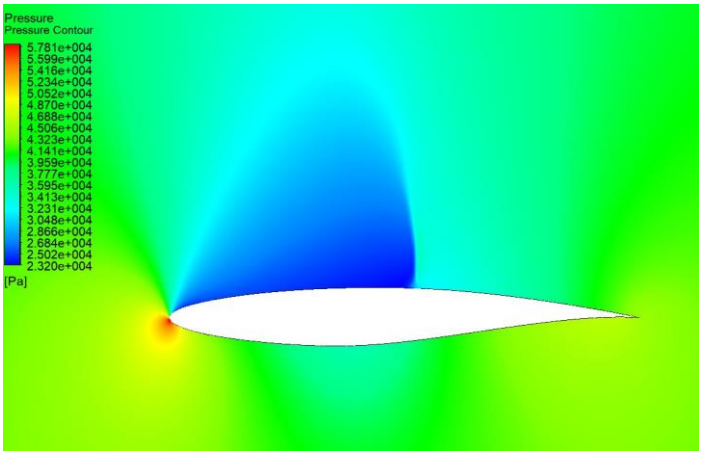

Fig. 8 Pressure Contour

The Mach number contour (Fig. 9) and velocity contour (Fig. 10) show the formation of localized supersonic flow. The zoomed in portion of the velocity contour in Fig. 10 shows the effect of shock on the boundary layer thickness. As a result of the adverse pressure gradient across the shock, the thickness of boundary layer increases. It indicates that the flow is critical and any increase in shock strength will increase the pressure gradient, as a result the boundary layer separates downstream of the shock.

International Journal of Engineering Research & Technology (IJERT)
ISSN: 2278-0181
Vol. 7 Issue 05, May-2018

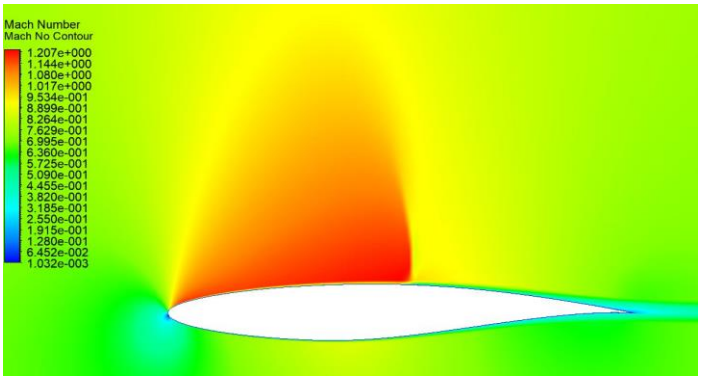

Fig. 9 Mach number contour

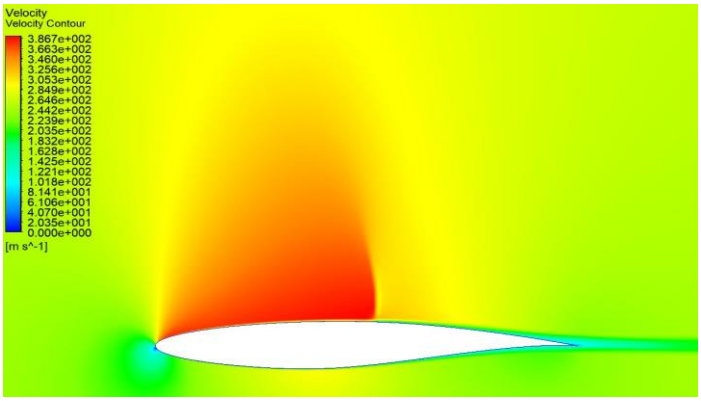

Fig. 10 Velocity Contour

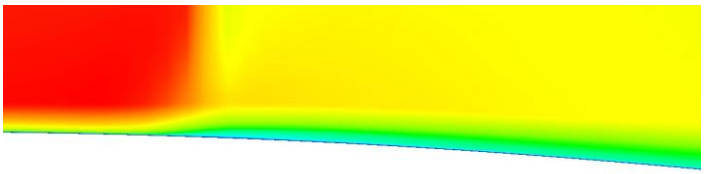

Fig. 11 Thickening of boundary layer aft of the shock

V. CONCLUSIONS

A grid independence study is carried out for RAE 2822 airfoil at a Mach number of 0.725 and Reynolds number of 6.5 million. A comparison of three different grid sizes shows that the results do not change with an increase in size of the grid. The pressure coefficient plot over the airfoil surface for all the three grids match with each other. The lift and drag coefficient values for the three grids are also compared which show that there is very less error. A comparison of pressure coefficient plots with the experimental values shows that the numerical results match well with the experimental results, although the shock location is predicted upstream of the experimental results. The Pressure contour and Mach number contour clearly show the formation of a normal shock on the upper surface of the airfoil. The Mach number contour also shows the formation of local supersonic flow over the upper surface of the airfoil indicating the freestream Mach number to be over the critical Mach number. The velocity contour shows the thickening of boundary layer aft of the shock wave indicating that any increase in flow conditions will lead to boundary layer separation.

REFERENCES

[1] Cook, P.H., M.A. McDonald, M.C.P. Firmin, Aerofoil RAE 2822-Pressure Distributions, and Boundary Layer and Wake Measurements, Experimental Data Base for Computer Program Assessment, AGARD Report AR 138, (1979)

[2] Anderson J.D., Introduction to Flight, New York, Tata Mcgraw Hill (2001)

[3] Anderson J.D., Introduction to Aerodynamics, New York, Tata Mcgraw Hill (2005)

[4] Anderson J.D., Fundamentals of Aerodynamics, Tata Mcgraw Hill (2007)

[5] Anderson J. D., Computational Fluid dynamics, New York, Tata Mcgraw Hill (1989)

[6] Menter F.R., Langtry R., Volker S., Transition Modelling for General Purpose CFD Codes, Flow Turbulence Combust, Springer Science (2006)